

Attraction and unbinding of like-charged rods (*)

A. NAJI^{1(**)}, A. ARNOLD², C. HOLM² and R. R. NETZ¹ (**)

¹ *Sektion Physik, LMU, Theresienstr. 37, D-80333 München, Germany.*

² *MPI für Polymerforschung, Ackermannweg 10, D-55128 Mainz, Germany.*

PACS. 87.15.-v – Biomolecules: structure and physical properties.

PACS. 61.20.Ja – Computer simulation of liquid structure.

PACS. 87.15.Nn – Properties of solutions; aggregation and crystallization of macromolecules.

Abstract. – We investigate the effective interaction between two like-charged rods in the regime of large coupling parameters using both Molecular Dynamics simulation techniques and the recently introduced strong-coupling theory. We obtain attraction between the rods for elevated Manning parameters accompanied by an equilibrium surface-to-surface separation of the order of the Gouy-Chapman length. A continuous unbinding between the rods is predicted at a threshold Manning parameter $\xi_c = 2/3$.

Introduction. – In recent years, both experiments [1] and numerical simulations [2–10] showed that like-charged macroions can attract each other via effective forces of electrostatic origin; one prominent example is the formation of dense packages of DNA molecules (DNA condensates) [1]. These observations indicate like-charge attraction in the presence of multi-valent counterions, at low temperatures or for large surface charge density on macroions, *i.e.* when electrostatic correlations between charged particles become increasingly important. The standard mean-field Poisson-Boltzmann (PB) theory predicts repulsion between like-charged objects [11]. In contrast, incorporation of electrostatic correlations generates attractive interactions in agreement with a variety of experimental and numerical results [12–22, 27]. The importance of electrostatic correlations can be quantified by means of the *coupling parameter*, $\Xi = 2\pi q^3 \ell_B^2 \sigma_s$, which depends on the charge valency of counterions, q , the surface charge density of macroions, σ_s , and the Bjerrum length, $\ell_B = e^2/(4\pi\epsilon\epsilon_0 k_B T)$ (associated with a medium of dielectric constant ϵ and at temperature T). The PB theory is valid in the limit of vanishingly small coupling parameter $\Xi \rightarrow 0$ [21–23], while non-mean-field features emerge in the opposite limit of large coupling, $\Xi \gg 1$, and are typically accompanied by the formation of strongly-correlated counterion layers. For charged *curved* surfaces, one has to consider the entropy-driven counterion-condensation process as well. For rod-like macroions, as considered in this paper, counterion condensation is controlled by the so-called *Manning parameter*, $\xi = q\ell_B\tau$ [24], where τ stands for the single-rod linear charge density (in units of the elementary charge e). For very small Manning parameter, ξ , counterions de-condense from the rods leading to a bare electrostatic repulsion between them [25]. For sufficiently large ξ , on the other hand, a certain fraction of counterions remains bound to the rods and attraction becomes possible for moderate to large couplings. We are interested in the regime of Manning parameters, ξ , and coupling parameters, Ξ , where an effective rod-rod attraction is present.

Several mechanisms for the attraction between like-charged rods have been considered in the literature, including covalence-like binding [26], Gaussian-fluctuation correlations [14],

(*) Revised version published in Europhys. Lett. **67**, 130 (2004).

(**) Present address: Physics Dept., Technical University of Munich, 85748 Garching, Germany.

and structural correlations [18–20]. The two latter approaches yield attraction based on correlated fluctuations of condensed counterions on opposite rods and short-ranged correlations due to the ground-state configuration of the system, respectively. Conflicting predictions for the threshold value of Manning parameter, above which attraction between two rods is possible, have been obtained: The analysis of Ray and Manning [26], based on the standard counterion-condensation model [24], leads to attraction for $\xi > 1/2$. In contrast, an attraction regime of $\xi > 2$ was proposed by the counterion-condensation theory of Arenzon *et al.* [20]. Recent numerical simulations [3, 10], on the other hand, reveal attraction already for Manning parameters of the order of $\xi \approx 1$ and for moderate coupling parameters, though did not specifically consider the threshold value of ξ . Recently, a systematic treatment of correlations in highly-coupled systems has been put forward [21], that employs a perturbative scheme (virial expansion) in terms of $1/\Xi$. This scheme leads to the asymptotic strong-coupling (SC) theory, which becomes exact in the limit which is complementary to the mean-field regime, *i.e.* when $\Xi \rightarrow \infty$. The SC theory has been used to study the interaction between planar charged walls [21] and shows quantitative agreement with Monte-Carlo simulations for moderate to large coupling parameters [22]. The SC mechanism of like-charge attraction qualitatively agrees with the structural-correlation scenario [17–20] for large macroion charges [21–23, 27]. In this letter, we study the effective interaction in a system of two like-charged rods using both Molecular Dynamics (MD) simulation methods and the SC theory. The nature of electrostatic correlations in such a system has been studied in our previous MD simulations [10], and exhibits a competition between electrostatic and excluded-volume interactions. Here, we focus on the strong-coupling characteristics of attraction between like-charged rods. In the following, these numerical results will be compared with the predictions of the SC theory [27].

Strong-coupling theory. – In the limit of large coupling parameter $\Xi \gg 1$, the canonical free energy of a system of fixed macroions with their neutralizing counterions, \mathcal{F} , admits a large-coupling expansion as $\mathcal{F} = \mathcal{F}_1/\Xi + \mathcal{F}_2/\Xi^2 + \dots$ [27], where the coefficients $\mathcal{F}_1, \mathcal{F}_2, \dots$ are expressed in terms of weighted integrals of Mayer functions over counterionic degrees of freedom, which are convergent for systems of counterions at charged macroscopic objects [21]. The first term in the above expression generates the leading non-vanishing contribution to statistical observables such as effective interaction between macroions for $\Xi \gg 1$; hence $\mathcal{F}_{\text{SC}} = \mathcal{F}_1/\Xi$ is referred to as the SC free energy of the system and \mathcal{F}_1 as the rescaled SC free energy. The SC free energy takes a very simple form in terms of the one-particle interaction energies between counterions and macroions (see, *e.g.*, eq. (1) below), and the mutual interaction between counterions themselves enters only in the sub-leading corrections [21, 27]. Physically, this reflects the fact that for $\Xi \rightarrow \infty$, counterions at charged objects are surrounded by an extremely large correlation hole and thus, the single-particle term becomes the dominant contribution [21–23, 27] (see also the discussion). Let us consider two infinitely long similar rods of length H and radius R that are located parallel at axial separation D in a rectangular box of lateral extension L containing also neutralizing counterions of valency q (fig. 1a). The rods are impenetrable to counterions and no additional salt is present. It is convenient to establish a dimensionless formalism for such systems by rescaling all length scales by the Gouy-Chapman length $\mu = 1/(2\pi q\ell_B\sigma_s)$, such as $\tilde{x} = x/\mu$, *etc.* [21], where $\sigma_s = \tau/(2\pi R)$ stands for the surface charge density of the rods. Clearly, the rod radius in rescaled units, $\tilde{R} = R/\mu$, coincides with Manning parameter, *i.e.* $\tilde{R} = \xi = q\ell_B\tau$. (We may occasionally use ξ or \tilde{R} to denote the Manning parameter.) The rescaled rod length, \tilde{H} , is related to the total number of counterions, N , via the global electroneutrality condition as $\tilde{H} = N\Xi/\xi$. The rescaled SC free energy of this system per rescaled unit length follows as [27]

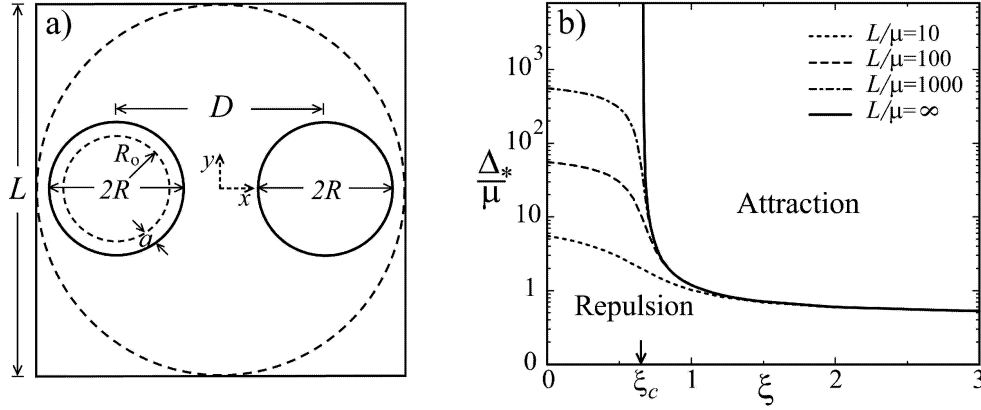


Fig. 1 – a) We consider two identical rods of radius R at axial distance D in an outer box of size L , which is rectangular (with square cross-section) in the analytical model and cylindrical in the simulations. R_0 and a are the Lennard-Jones potential parameters defined in the simulation model. b) The rescaled equilibrium surface-to-surface distance of rods, $\tilde{\Delta}_* = \Delta_*/\mu = (D_* - 2R)/\mu$, obtained from the SC theory as a function of Manning parameter, $\xi = q\ell_B\tau$, for various rescaled box sizes, L/μ , indicated on the graph. In the infinite-box limit, a continuous unbinding occurs at $\xi_c = 2/3$.

$$\frac{\mathcal{F}_1}{\tilde{H}} = -2\xi^2 \ln \tilde{D} - 2\xi \ln \left[\int_V d\tilde{x}d\tilde{y} \tilde{r}_1^{-2\xi} \tilde{r}_2^{-2\xi} \right]. \quad (1)$$

The integral runs over the volume V available for counterions within the confining box, excluding the rods. We defined $\tilde{r}_{1,2} = [(\tilde{x} \pm \tilde{D}/2)^2 + \tilde{y}^2]^{1/2}$ as the radial distances from the rods axes. The first term in eq. (1) is nothing but the bare electrostatic repulsion between the rods. The second term involves the leading (energetic and entropic) contributions from counterions, which leads to a counterion-mediated attraction between sufficiently highly charged rods [29]. This term also reflects the de-condensation process of counterions at low Manning parameters: For $\xi < 1/2$, the counterionic integral in eq. (1) diverges in the infinite-volume limit $\tilde{L} \rightarrow \infty$, hence the distribution of counterions around the rods and the counterion-mediated force vanish, *i.e.* the rods purely repel each other [25]. For large Manning parameter $\xi \gg 1$, on the other hand, the rescaled SC free energy, \mathcal{F}_1 , shows a long-ranged attraction and a pronounced global minimum at a small axial separation $\tilde{D}_* \approx 2\tilde{R}$, which is nothing but the equilibrium axial separation of the rods [27]. For $\xi \gg 1$, the counterionic distribution becomes strongly localized in a narrow region between the rods, indicating that the SC attraction is accompanied by strong accumulation of counterions in the intervening region. This allows for a saddle-point calculation of the counterionic integral in eq. (1), giving the approximate form of \mathcal{F}_1 in the vicinity of its local minimum as [27]

$$\mathcal{F}_1/\tilde{H} \approx 6\xi^2 \ln \tilde{D} - 2\xi \ln(\tilde{D} - 2\tilde{R}). \quad (2)$$

The equilibrium surface-to-surface distance of the rods for large ξ is obtained by minimizing expression (2) as $\tilde{\Delta}_* \equiv \tilde{D}_* - 2\tilde{R} \approx 2/3 + \mathcal{O}(1/\xi)$, which corresponds, in real units, to a surface separation of the order of the Gouy-Chapman length, μ [31]. Figure 1b shows the global behavior of the rescaled equilibrium surface-to-surface distance, $\tilde{\Delta}_*$, obtained by numerical minimization of the full SC free energy, eq. (1), as a function of ξ for several box sizes. For large ξ , attraction is dominant, the rods form a closely-packed bound state, and the volume of the bounding box is irrelevant due to strong condensation of counterions. However,

for decreasing ξ , attraction is weakened and rods eventually unbind in a continuous fashion when $\tilde{L} \rightarrow \infty$. For two unconfined rods (solid curve in fig. 1b), the unbinding transition occurs at $\xi_c = 2/3$ and exhibits an asymptotic power-law behavior as a function of the reduced Manning parameter as $\tilde{\Delta}_* \sim (\xi - 2/3)^{-\alpha}$, where $\alpha \approx 3/2$ [27]. Note that the predicted onset of rod-rod attraction, $\xi_c = 2/3$, is somewhat larger than the counterion-condensation threshold for the combined system of two rods, $\xi = 1/2$ [26], and smaller than the condensation threshold for a single rod, $\xi = 1$ [24]. This reflects the subtle crossover from the case of two coupled rods (when the distance between them is small) to the case of two decoupled rods as the axial distance diverges when the unbinding threshold is approached. The predicted attractive force between rods, $F_{\text{rods}} = -(k_B T) \partial \mathcal{F}_{\text{SC}} / \partial D$ (in actual units), is found from eq. (2) to be inversely proportional to the axial distance, D . This force increases and tends to a temperature-independent value upon increasing ξ (or decreasing temperature) [3], which is nothing but the *energetic attraction* mediated by counterions sandwiched between closely-packed rods, *i.e.* $F_{\text{rods}} = -3e^2\tau^2/(2\pi\epsilon\epsilon_0 D)$ [27]. The SC attraction for large ξ , thus, originates from the energetic contributions induced by the ground-state configuration of counterions and in this respect, agrees qualitatively with the low-temperature picture for like-charge attraction [17–20]. Though for the specific case of two charged rods, the quantitative predictions of the SC theory for the (energetic) inter-rod force at large ξ , and for the attraction threshold differ from the results of the model studied in ref. [20], which incorporates a discrete charge pattern for the rods and obtains attraction for $\xi > 2$ [20].

Simulation method. – To study the interaction between two like-charged rods numerically, we have performed extensive Molecular Dynamics simulations making use of a Langevin thermostat to drive the system into the canonical state. The geometry of the simulated system is similar to what we have sketched in fig. 1a; the outer confining box is here chosen to be cylindrical. Other parameters are defined in the same way unless explicitly mentioned. Charged particles interact via bare Coulombic interaction and excluded-volume interactions. We apply periodic boundary conditions in the direction parallel to the rods axes. This leads to summation of infinite series for Coulomb interaction over all periodic images, which is handled numerically using the MMM1D summation method [30]. As we are only interested in examining electrostatic aspects of the effective rod-rod interaction, excluded-volume interactions are considered only between rods and counterions and not between counterions themselves. (Extended numerical results with excluded-volume interaction between counterions will be presented elsewhere [28].) We employ a shifted Lennard-Jones potential as

$$V_{\text{LJ}}(r) = \begin{cases} 4\epsilon \left[\left(\frac{a}{r-R_0} \right)^{12} - \left(\frac{a}{r-R_0} \right)^6 + \frac{1}{4} \right] & : (r - R_0) < 2^{1/6}a, \\ 0 & : \text{otherwise} \end{cases}, \quad (3)$$

where R_0 is an offset used to control the radius of the rods, a defines our basic length scale in the simulations, and $\epsilon \approx 1k_B T$. Therefore, $R = R_0 + a$ may be regarded as the effective rod radius and is directly compared with the SC result (with hard-core rods). This is justified since in the simulations only a negligible fraction of counterions penetrates the above potential to reach radial distances smaller than R . In the simulations, the diameter of the (cylindrical) outer box is chosen as $8D$. For the final comparison (fig. 2), the theoretical curves are also calculated using a similar constraint, though for simplicity and as explained before, calculations have been done for a square box of edge size $L = 8D$. As we have explicitly checked, the results are insensitive to small changes in the box size for the considered range of Manning parameter (see also fig. 1b), and the SC predictions can thus be compared with the simulations. To obtain the location of the zero-force (equilibrium) point in the force curves,

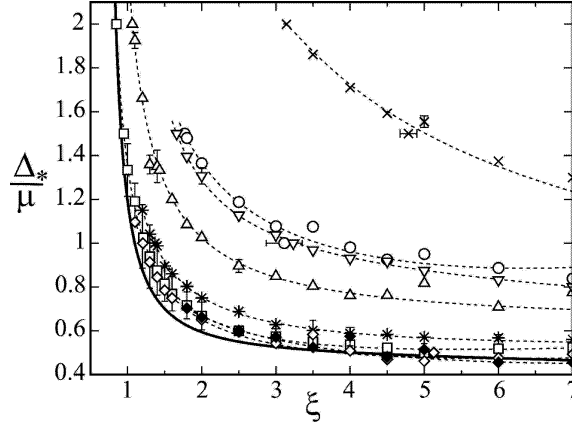


Fig. 2 – The equilibrium surface-to-surface distance of two rods in rescaled units, $\tilde{\Delta}_* = \Delta_*/\mu = (D_* - 2R)/\mu$, as a function of Manning parameter, $\xi = q\ell_B\tau$. Symbols show simulation results for (from top): $\gamma_{RB} = 3$ (crosses), 9.1 (open circles), 10 (open triangle-downs), 15 (open triangle-ups), 30 (stars), 40 (open squares), 50 (open diamonds), 60 (filled diamonds). The solid curve is the SC prediction obtained by numerical minimization of eq. (1). Dashed curves are guides to the eye.

we have employed a bisection algorithm followed by a linear regression. The error bars are determined from the error of the linear regression using the error propagation method.

Results and discussion. – To clearly separate the attraction and repulsion regimes of two like-charged rods numerically, we study the rescaled equilibrium surface-to-surface separation of rods, $\tilde{\Delta}_*$, as a function of Manning parameter, ξ , in our simulations. The results will then be compared with the SC prediction (fig. 1b). To this end, we fix the actual surface-to-surface distance between the rods, $\Delta = D - 2R$, and their linear charge density, τ , together with the counterion valency, q , but vary the Bjerrum length, ℓ_B , and the actual rod radius, R . By doing so, the Gouy-Chapman length associated with this system, $\mu = R/(\ell_B q \tau)$, is varied, which then allows for determining the equilibrium surface-to-surface separation *in rescaled units*, $\tilde{\Delta}_* = \Delta_*/\mu$. The results will also depend upon the electrostatic coupling parameter, $\Xi = 2\pi q^3 \ell_B^2 \sigma_s$, which is finite in the simulations and may be written as

$$\Xi = \xi \tilde{\Delta} \gamma_{RB}, \quad (4)$$

where $\gamma_{RB} = q/(\tau\Delta)$ is a dimensionless parameter referred to here as the *Rouzina-Bloomfield parameter* (see the discussion below). The simulation results for the equilibrium surface-to-surface separation of the rods are shown in fig. 2 for different γ_{RB} ranging from 3 to 60. The data have been obtained using various combinations of fixed $\tau a = 1.0, 0.33, 0.10$, $q = 1, 3, 5, 10$ and $\Delta/a = 0.5, 1.0, 2.0, 2.5$. For a given set of system parameters (τ , q and Δ) chosen in the simulations, γ_{RB} is fixed and identifies a single curve. As seen, upon increasing the Rouzina-Bloomfield parameter, γ_{RB} , the equilibrium separation decreases indicative of a stronger attraction operating between the rods, and at the same time, the agreement between simulation data and the SC prediction (solid curve in fig. 2) becomes progressively better. The agreement is quantitative for large γ_{RB} , *i.e.* $\gamma_{RB} = 50$ and 60. (The data set with $\gamma_{RB} = 60$ is obtained using $q = 3$, $\tau a = 0.1$ and $\Delta/a = 0.5$, and data with $\gamma_{RB} = 50$ are obtained using $q = 5$, $\tau a = 0.1$ and $\Delta/a = 1.0$.) The observed trend for increasing γ_{RB} is associated with the increase of the coupling parameter, Ξ , in the simulated system (see eq. (4)), which eventually exhibits the strong-coupling regime. (For instance, for a moderate Manning parameter of $\xi = 3.0$, Ξ increases from 18 for cross symbols up to about 100 for filled diamonds.)

It is noteworthy that γ_{RB} , as defined above, can be expressed as $\gamma_{\text{RB}} = \delta/\Delta$, where $\delta = q/\tau$ is the projected distance between counterions along a single rod as follows from the local electroneutrality condition. Note that δ roughly gives the correlation hole size around counterions at charged surfaces [6, 7, 10, 22, 23]. The appearance of strong attractive forces for $\gamma_{\text{RB}} > 1$ was first addressed by Rouzina and Bloomfield [17] for a system of two planar charged walls. Analytical and numerical results for planar walls [21–23] have in fact shown that the *relative* magnitude of higher-corrections to the asymptotic SC theory decreases with γ_{RB} , and the SC regime at finite Ξ is characterized by the Rouzina-Bloomfield criterion $\gamma_{\text{RB}} > 1$. Physically, this corresponds to a large correlation hole size around counterions at macroion surfaces as compared with the macroions surface separation, *i.e.* $\delta > \Delta$, leading to a dominant contribution from single (isolated) counterions [21–23], which is formally obtained within the SC scheme [21]. It becomes exceedingly difficult to perform systematic analytic calculations to examine higher-order corrections to SC predictions given the geometry of the two-rod system. Nonetheless, the present numerical results clearly indicate a qualitatively similar trend for increasing γ_{RB} in this system and that, the SC regime is characterized by Rouzina-Bloomfield criterion. Due to convergence limitations, our numerical investigation so far has been limited to the range of $\xi > 0.8$ and thus do not cover the close vicinity of the unbinding transition. (It becomes more difficult to obtain good data as the rods equilibrium distance rapidly increases for small ξ .) However, the excellent convergence of the simulation results to the asymptotic SC prediction suggests an attraction threshold of about $\xi_c = 2/3$ for two rods in the strong-coupling limit as obtained using the SC theory. Note that for small Manning parameters where counterions de-condense ($\xi \leq 1/2$), electrostatic correlations are suppressed due to entropic dilution of the counterionic cloud. Physically, this regime does not exhibit strong energetic coupling and higher-order corrections to the SC theory may become important. Nevertheless as we showed, the SC theory captures the de-condensation process and leads to a qualitatively consistent picture for the whole range of Manning parameters [25]. (Note that the predicted onset of de-condensation at $\xi = 1/2$ and also the bare macroionic repulsion for small ξ *quantitatively* agree with previous findings [26].) How and whether the predicted attraction threshold ($\xi_c = 2/3$) and the unbinding behavior is influenced by the de-condensation process of counterions at small ξ remains to be clarified.

In summary, we have investigated the attraction and repulsion regimes of two like-charged rods in terms of Manning parameter, ξ , and the coupling parameter, Ξ , by combining numerical and analytical approaches. For large ξ , the rods form a closely-packed bound state of small surface-to-surface separation of about the Gouy-Chapman length, μ [31]. The attraction is weakened and the rods unbind for decreasing ξ . The attraction threshold is found at $\xi_c = 2/3$, and the unbinding of rods proceeds in a continuous fashion characterized by a power-law for the rods surface separation, $\Delta_* \sim (\xi - 2/3)^{-\alpha}$, with an exponent $\alpha \approx 3/2$. The predicted attraction regime for large ξ is accessible experimentally using, *e.g.*, DNA molecules ($\tau e \approx 6 e/\text{nm}$) in the presence of multivalent counterions such as spermidine ($q = 3$), which yields $\xi \approx 12$ and $\Xi \approx 80$. For these values, our results predict attraction with an equilibrium surface separation $\Delta_* \sim \mu$, where for the DNA-spermidine system $\mu \sim 1 \text{ \AA}$ [31]. It should be noted, however, that for DNA-like molecules (large τ), other factors such as excluded-volume interaction between counterions [10, 28] and the helical structure of DNA [18, 19] may become important and contribute additional components to the total effective force. The predicted continuous unbinding occurs at quite small values of Manning parameter. Experimentally, this phenomenon could be studied with weakly charged stiff polymers, such as poly-phenylene with a suitably chosen small density of charged side-chains. The effects of salt can be qualitatively accounted for by associating the bounding box size with the screening length: Thus only close to the unbinding do we expect addition of salt to matter. The effects of finite chain

stiffness and the bundling of many chains constitute interesting applications for the future.

A.N. and R.R.N. acknowledge funds from DFG German-French Network. C.H. and A.A. acknowledge funds from the Zentrum für Multifunktionelle Werkstoffe und Miniaturisierte Funktionseinheiten, grant BMBF 03N 6500, DFG grant Ho 1108/11-1, and SFB 625.

REFERENCES

- [1] V. Bloomfield, *Biopolymers* **31**, 1471 (1991); H. Strey et al., *Curr. Opin. Struct. Biol.* **8**, 309 (1998); M. Olvera de la Cruz et al., *J. Chem. Phys.* **103**, 5781 (1995); J. X. Tang et al., *Ber. Bunsen-Ges. Phys. Chem.* **100**, 1 (1996); J. C. Butler et al., *Phys. Rev. Lett.* **91**, 028301 (2003).
- [2] L. Guldbrand, B. Jönsson, H. Wennerström, P. Linse, *J. Chem. Phys.* **80**, 2221 (1984); L. Guldbrand, L. G. Nilsson, and L. Nordenskiöld, *J. Chem. Phys.* **85**, 6686 (1986); A. P. Lyubartsev and L. Nordenskiöld, *J. Phys. Chem.* **99**, 10373 (1995).
- [3] N. Grønbech-Jensen, R. Mashl, R. Bruinsma, and W. Gelbart, *Phys. Rev. Lett.* **78**, 2477 (1997).
- [4] N. Grønbech-Jensen, K. M. Beardmore, P. Pincus, *Physica A* **261**, 74 (1998).
- [5] J. W. Wu, D. Bratko, and J. M. Prausnitz, *Proc. Natl. Acad. Sci. USA* **95**, 15169 (1998).
- [6] E. Allahyarov, I. D'Amico, and H. Löwen, *Phys. Rev. Lett.* **81**, 1334 (1998).
- [7] P. Linse and V. Lobaskin, *Phys. Rev. Lett.* **83**, 4208 (1999); *J. Chem. Phys.* **112**, 3917 (2000).
- [8] M. J. Stevens, *Phys. Rev. Lett.* **82**, 101 (1999).
- [9] R. Messina, C. Holm, and K. Kremer, *Phys. Rev. Lett.* **85**, 872 (2000).
- [10] M. Deserno, A. Arnold, and C. Holm, *Macromolecules* **36**, 249 (2003).
- [11] E. J. Verwey and J. T. G. Overbeek, *Theory of the stability of lyophobic colloids* (Elsevier, Amsterdam, 1948); J. C. Neu, *Phys. Rev. Lett.* **82**, 1072 (1999).
- [12] R. Kjellander and S. Marčelja, *J. Chem. Phys.* **82**, 2122 (1985).
- [13] P. Attard, D. J. Mitchell, and B. W. Ninham, *J. Chem. Phys.* **88**, 4987 (1988); R. Podgornik, *J. Phys. A: Math. Gen.* **23**, 275 (1990); P. A. Pincus and S. A. Safran, *Europhys. Lett.* **42**, 103 (1998); D. B. Lukatsky and S. A. Safran, *Phys. Rev. E* **60**, 5848 (1999); M. Kardar and R. Golestanian, *Rev. Mod. Phys.* **71**, 1233 (1999); A. W. C. Lau and P. Pincus, *Phys. Rev. E* **66**, 041501 (2002); A. W. C. Lau, D. Levine, and P. Pincus, *Phys. Rev. Lett.* **84**, 4116 (2000).
- [14] F. Oosawa, *Biopolymers* **6**, 1633 (1968); J.-L. Barrat and J.-F. Joanny, *Adv. Chem. Phys.* **XCIV**, 1 (1996); B.-Y. Ha and A. J. Liu, *Phys. Rev. Lett.* **79**, 1289 (1997); R. Podgornik and V. A. Parsegian, *Phys. Rev. Lett.* **80**, 1560 (1998).
- [15] M. J. Stevens and M. O. Robbins, *Europhys. Lett.* **12**, 81 (1990).
- [16] M. C. Barbosa, M. Deserno, and C. Holm, *Europhys. Lett.* **52**, 80 (2000).
- [17] I. Rouzina and V. A. Bloomfield, *J. Phys. Chem.* **100**, 9977 (1996).
- [18] A. Kornyshev and S. Leikin, *J. Chem. Phys.* **107**, 3656 (1997); *Phys. Rev. Lett.* **82**, 4138 (1999).
- [19] B. I. Shklovskii, *Phys. Rev. Lett.* **82**, 3268 (1999); A. Yu. Grosberg, T. T. Nguyen, and B. I. Shklovskii, *Rev. Mod. Phys.* **74**, 329 (2002).
- [20] J. J. Arenzon, J. F. Stilck, and Y. Levin, *Eur. Phys. J. B* **12**, 79 (1999); Y. Levin, *Rep. Prog. Phys.* **65**, 1577 (2002).
- [21] R. R. Netz, *Eur. Phys. J. E* **5**, 557 (2001).
- [22] A. G. Moreira and R. R. Netz, *Phys. Rev. Lett.* **87**, 078301 (2001); *Eur. Phys. J. E* **8**, 33 (2002).
- [23] Y. Burak, D. Andelman and H. Orland, *Phys. Rev. E* **70**, 016102 (2004).
- [24] G. S. Manning, *J. Chem. Phys.* **51**, 924 (1969).
- [25] The de-condensation process at small ξ occurs in the whole range of coupling parameters and does not exhibit energetic strong-coupling characteristics (Naji and Netz, preprint (2004)).
- [26] J. Ray and G. S. Manning, *Macromolecules* **30**, 5739 (1997); *Langmuir* **10**, 2450 (1994).
- [27] A. Naji and R. R. Netz, *Eur. Phys. J. E* **13**, 43 (2004).
- [28] A. Arnold and C. Holm, to be published.
- [29] Note that the translational entropy of the rods is irrelevant for large rod length.

- [30] A. Arnold and C. Holm, *Comp. Phys. Comm.* **148**, 327 (2002).
- [31] The SC results hold for arbitrary counterion size, when hard-core interactions are taken into account. In this case, R measures the distance of closest approach between rods and counterions, and the equilibrium surface separation of rods (in actual units) is found to increase by an amount equal to the counterion diameter [27].